degrees of ionization. The results of these studies will be reported elsewhere.[20]

Acknowledgment. The authors are deeply indebted to Professor F. Quadrifoglio for discussions during this work, and to Professors M. Mammi and V. Crescenzi for critical reading of the manuscript. The work was carried out with the financial support of the Institute of Macromolecular Chemistry of Milan, Italy.

(20) Just before submitting our manuscript for publication, a paper by Myer and Barnard appeared: Y. P. Myer and E. A. Barnard, *Arch. Biochem. Biophys.*, **143**, 116 (1971). These authors determined CD spectra of a commercial sample of PLH at various pH values and found a pH-induced conformational transition. A direct comparison of their data with our data cannot be made since these authors did not report spectra as a function of the significant variable, that is, the degree of protonation of the polymer side chains. However, the CD pattern reported in our work at α near 0.9 is very much the same as that reported by Myer and Barnard at pH near 6 (where deprotonation should be essentially complete) except for band intensity: the CD bands reported in our work are much more intense than those measured by the above-mentioned authors. We have observed (see the Experimental Section) that spectra with low band intensities are obtained when the PLH sample does contain substantial amounts of low molecular weight material. After exhaustive dialysis, which eliminates the low molecular weight fraction, normal spectra are obtained.

The results obtained by us in the 222-nm region are not in accord with those of the above-mentioned authors. We have carried out a number of measurements (see Figure 5) using 5-mm path-length cells in order to obtain large CD signals and minimize the errors. No clear transition appeared on varying the degree of protonation of the polymer side chains, and we therefore concluded that the variation of the spectrum in this region is mainly sensitive to changes of the protonation extent of the side chains.

From the CD spectral characteristics, the above-mentioned authors infer that PLH assumes the β form at a low degree of protonation of the imidazole side chains. This statement is not in conflict with our copolymer studies which exclude only the existence of the right-handed α helix. However, we stress the point that the presence of the side-chain chromophores prevents a safe interpretation of the CD pattern in terms of conformation. The fact that in the solid state PLH has been found in the β form does not necessarily mean that the same conformation exists in solution. As previously discussed, the solid-state conformation is strongly dependent on the "history" of the solid sample. For instance, Zundel and coworkers[18] found the α-helical form on films of PLH.

In conclusion, we believe that additional studies are needed in order to establish *unambiguously* the exact conformation of charge-free PLH in solution.

Polymer–Solvent Interactions for Homopolypeptides in Aqueous Solution

A. J. Hopfinger

Division of Macromolecular Science, Case Western Reserve University, Cleveland, Ohio 44106. *Received June 1, 1971*

ABSTRACT: A polymer–solvent interaction model, based upon the concept of a hydration shell, is used to evaluate the free energy of solvation of many different homopolypeptides in aqueous solution. The solvation free energy is roughly proportional to the solubility of the macromolecule, and the interactions of polar groups with aqueous solvent are more stabilizing than the interactions of hydrophobic groups with aqueous solvent are destabilizing. Polymer–solvent interactions and intrachain–side chain interactions make the major energetic contributions to the helix $\rightleftharpoons$ coil transition. The aqueous solution–homopolypeptide interactions are moderately sensitive to conformation and the right-handed α helix has the least favorable polymer–solvent free energy interaction.

The conformation of a macromolecule is dependent upon the medium in which it exists. For example, the conformation of a macromolecule in the solid state is dependent upon how it packs with other macromolecules in the crystal. In fact, the intermolecular configurational energy which results from all the pairwise interactions of atoms belonging to different macromolecules can be the same magnitude as the intramolecular conformational energy which results from all the pairwise interactions of the nonbonded atoms within a single macromolecule.[1] In a similar way one would expect to observe strong polymer–solvent interactions for certain polymers in certain solvents. That this is the case follows from experiments in which variations in solvent composition (*i.e.*, changes in pH, salt concentration, polarity, and binary solvent mixtures)[2–6] have been shown to induce specific conformational changes in macromolecules.

A major criticism of theoretical conformational calculations has been the neglect of these polymer–solvent interactions in the computations. In the past, the implicit assumption has been made that a stable conformation in a vacuum would also be stable in any of a number of solvents. In view of experimental data, this assumption apparently oversimplifies the true situation. The purpose of this paper is to (i) report the development of a polymer–solvent interaction model in which the parameters of the model have been evaluated for aqueous solution at room temperature, (ii) elucidate the role of polymer–solvent interactions on the conformational stability of several different types of homopolypeptides in aqueous solution, (iii) provide an energetic explanation of the helix $\rightleftharpoons$ coil transitions observed in some homopolypeptides which possess ionizable side chains.

Polymer–polymer interactions were not included in the calculations. Thus, the results reported in this paper should only be valid for very dilute aqueous solutions and/or dilute "neutral solvent" solutions in which the solvent molecules are nearly spherical and have small effective volumes. Since polymer–solvent interactions depend upon the shape of the solvent molecule as well as its effective polarity, care should be taken in any attempt to rationalize the behavior of various nonaqueous solvents in terms of the data presented in this paper.

(1) A. J. Hopfinger, *Biopolymers*, **10**, 1299 (1971).
(2) P. Doty and J. T. Yang, *J. Amer. Chem. Soc.*, **81**, 2499 (1959).
(3) E. R. Blout, P. Doty, and J. T. Yang, *ibid.*, **79**, 749 (1957).
(4) G. D. Fasman, C. Lindblow, and E. Bodenheimer, *Biochemistry*, **3**, 155 (1964).
(5) H. Noguchi and J. T. Yang, *Biopolymers*, **1**, 359 (1963).
(6) J. S. Franzen, C. Bobik, and J. B. Harry, *ibid.*, **4**, 637 (1966).

Theory

Polymer–Solvent Hydration Shell Model. The concept of a hydration shell to describe the behavior of solvent molecules near a solute species has been used for many years.[7] Gibson and Scheraga[8] modified existing hydration shell models so as to be applicable to the atoms of a solute macromolecule. The model used in this report is a further modification of the basic hydration shell concept. It differs from the Gibson–Scheraga model in the size and properties of the hydration shells and the criteria for calculating excluded volumes in the hydration shells.

The concept of a hydration shell implies that a characteristic sphere can be centered about each atom of the macromolecule the size of which is dependent upon the solvent molecule and solute atom of the macromolecule. A particular change in free energy is associated with the removal of a solvent molecule from the hydration shell. The size of the hydration shell and the shape of the solvent molecule dictate how many solvent molecules can occupy the hydration shell. The sum of the intersections of the van der Waals volumes of the atoms of the macromolecule with the hydration sphere results in an excluded hydration shell volume which determines how many solvent molecules are removed from the hydration shell when the macromolecule is in a particular conformation. Thus the hydration shell is sensitive to conformation *via* excluded hydration shell volumes.

The hydration shell model is a four-parameter system in which n = the maximum number of solvent molecules which can occupy the hydration shell, Δf = the change in free energy associated with the removal of one solvent molecule from the hydration shell, R_v = the effective radius of the hydration shell, and V_f = the free volume of packing associated with one solvent molecule in the hydration shell.

Table I contains the values of the parameters n, Δf, R_v, and V_f for several different atoms solvated in aqueous solution. Also given in Table I are the values for each V_i', which is defined as the effective volume of the hydration shell of atom i. This quantity must be known in order to compute V_f, and, in itself, is a useful parameter for measuring the "amount of room" which solvent molecules can occupy about atom i of the macromolecule. Perhaps the best way to explain how the values of the hydration shell parameters are calculated is to describe the computational procedure for a representative case.

TABLE I
THE MACROMOLECULE–SOLVENT INTERACTION PARAMETERS R_v, V_f, n, AND Δf FOR SOME ATOMS IN AN AQUEOUS SOLUTION[a]

Atom or group	n	Δf, kcal/mol	R_v, Å	V_f, Å^3	V', Å^3
N(sp^2)	2	0.63	4.33	35.8	114.0
C(sp^2)	2	0.63	3.90	14.3	71.0
O(carbonyl)	2	1.88	3.94	67.6	177.6
H(amide)	2	0.31	3.54	31.3	105.0
CH_3(aliphatic)	8	−0.13	5.50	41.8	498.2
CH_2(aliphatic)	4	−0.10	5.50	60.8	328.0
CH(aliphatic)	2	−0.13	5.50	104.8	252.0
CH(aromatic)	3	0.11	3.90	3.3	76.6
O(hydroxyl)	2	1.58	3.94	55.2	152.8
H(hydroxyl)	2	0.31	3.54	54.7	151.8
O^-(carboxyl)	4	4.20	4.10	42.5	255.0
O(carboxyl)	2	4.20	4.10	64.1	170.6
H(carboxyl)	2	0.31	3.54	54.7	151.8

Volume of the H_2O molecule V_s = 21.2 Å^3

[a] Also given here is V', the effective hydration shell volume.

For example, the values of n, R_v, V_f, and V' were calculated for N(sp^2) as follows. First, a bonding geometry was assigned to the N(sp^2) atom by choosing a sphere having the van der Waals radius of nitrogen (1.35 Å)[9] to represent the bulk of the atom. Then, to account for the trigonal covalent bonds in which the N(sp^2) atom participates, three cylinders of indefinite length having radii equal to three-quarters the radius of the sphere were positioned around the van der Waals sphere in threefold symmetry. The radius of the cylinders were determined from studying Corey–Pauling–Koltun (CPK) molecular models of N(sp^2). The sphere and cylinders represented an infinite potential barrier to the solvent molecules. Solvent molecules were assigned initial positions about this model for the N(sp^2) atom and the total interaction energy of the system, including interactions between the N(sp^2) atom and solvent molecules as well as solvent molecule–solvent molecule interactions, was minimized using the Davidon technique.[10] The conformational potential functions and parameters used in several other investigations[11–14] were employed to calculate the total interaction energy for each iteration in the minimization. Whenever possible, use was made of the symmetry of the model in order to reduce the number of variables to be minimized. Since the N(sp^2) atomic geometry possessed a twofold plane of symmetry (the plane being defined by the axes of the cylinders), solvent molecules were added to the system in pairs, one on each side of the plane, having mirror positions and orientations relative to one another. In order to restrict the calculations to a single hydration shell, the constraint was imposed that only those minima in potential energy were considered which corresponded to positions and orientations of the solvent molecules within a distance equal to the sum of the van der Waals radius for the N(sp^2) atom plus the steric diameter of a water molecule (3.7 Å from CPK models). This distance represents an initial upper-limit approximation for the radius of the first hydration shell of the N(sp^2) atom.

The volume, V_s, of the solvent molecule (in this case water) was calculated by assigning van der Waals spheres[9] to represent the oxygen and two hydrogens and determining how much volume these three spheres manifested when they were allowed to overlap in a manner consistent with the bond lengths and bond angle of the H_2O molecule. Equation 5 was used to make this volume calculation, and V_s for H_2O is given in Table I.

Values of n equal to 2, 4, 6, and 8 were used in the energy minimization. The results indicated that n = 2 yielded the deepest energy minimum, and the two water molecules positioned and orientated themselves about the N(sp^2) atom in such a manner that the effective hydration shell radius, R_v, is 4.33 Å. Next the value of V' was computed by subtracting the volumes of the van der Waals sphere and the three cylinders of the N(sp^2) model from the hydration shell volume of the N(sp^2) atom using R_v as the hydration shell radius. Then V_f could be computed from

(7) E. A. Moelwyn-Hughes, "Physical Chemistry," Pergamon Press, Elmsford, N. Y., 1957.
(8) K. D. Gibson and H. A. Scheraga, *Proc. Nat. Acad. Sci. U. S.*, **58**, 420 (1967).
(9) A. Bondi, *J. Phys. Chem.*, **68**, 441 (1964).
(10) W. C. Davidon, AEC Research and Development Report No. ANL-5090, 1959.
(11) A. J. Hopfinger and A. G. Walton, *Biopolymers*, **9**, 29 (1970).
(12) A. J. Hopfinger and A. G. Walton, *ibid.*, **9**, 433 (1970).
(13) F. R. Brown, A. J. Hopfinger, and E. R. Blout, *J. Mol. Biol.*, in press.
(14) K. A. Mauritz and A. J. Hopfinger, in preparation.

$$V_f = (V' - nV_s)/n \quad (1)$$

The Δf values are taken from the work of Gibson and Scheraga[8] rather than using the potential energies found in the energy minimizations from which the n, R_v, and V_f were determined. There are two reasons for doing this: (a) Gibson and Scheraga report *free* energies rather than internal energies as were found in the energy minimizations and (b) the Gibson–Scheraga parameters were found experimentally and, hence, are probably more accurate than the theoretical predictions. It is interesting to note, however, that no theoretical interaction energy between polymer atom and solvent molecule differs from the corresponding free energy interaction as given by Gibson and Scheraga by more than 12%. Using analogous procedures to those presented for the N(sp^2) atom, it was possible to evaluate the necessary polymer–solvent interaction parameters for the atomic species listed in Table I.

To complete the polymer–solvent interaction model, the following properties are assigned to the hydration shells. (i) The solvent molecules occupy identical volume ($V_s + V_f$) in a hydration shell, which are independent of how many other solvent molecules are present at any instant. (ii) The dynamic characteristics of the polymer–solvent interaction are included by assuming a linear relationship between the total change in free energy and the amount of excluded volume in the hydration shell. (iii) There is no additional contribution to the polymer–solvent free energy from a hydration shell once n solvent molecules have been removed from the hydration shell. (iv) All energy parameters are valid only for room temperature. There are three unique types of intersections between the hydration shell of atom i and the van der Waals sphere of atom j having volume V_j and radius r_j: (a) $V_i' \cap v_j = 0$ when $R_{vi} + r_j \leq r_{ij}$, where r_{ij} is the distance between the centers of atoms i and j; (b) $V_i' \cap v_j = (4/3)\pi r_j^3$ when $r_j + r_{ij} \leq R_{vi}$; (c) the third case is $R_{vi} + r_j > r_{ij}$. With the aid of Figure 1 we can derive an expression for $V_i' \cap v_j$. First we compute the volume associated with $V_i' \cup v_j$ by the solid of revolution technique which is described in any elementary calculus text.

From simple analytic geometry, it is found that the x coordinate, x^*, of the intersection of the solvation shell and the van der Waals sphere is given by

$$x^* = (R_{vi}^2 - r_j^2 + r_{ij}^2)/2r_{ij} \quad (2)$$

Then for $r_j + R_{vi} > r_{ij}$

$$V_i' \cup v_j = \pi\left[\int_{-R_{vi}}^{x^*}(R_{vi}^2 - \chi^2)d\chi + \int_{x^*}^{r_i+r_{ij}}(r_j^2 - [\chi - r_{ij}]^2)d\chi\right] \quad (3)$$

and

$$V_i' \cap v_j = (4/3)\pi(R_{vi}^3 + r_j^3) - V_i' \cup v_j \quad (4)$$

or

$$V_i' \cap v_j = (\pi/3)[2R_{vi}^3 + 2r_j^3 + r_{ij}^3] - \pi[R_{vi}^2 x^* + (r_{ij} - x^*)(r_j^2 + r_{ij}x^*)] \quad (5)$$

Then for some particular conformation, K, of the macromolecule having a total of N atoms, the total excluded volume of the ith hydration shell due to all other nonbonded atoms is

$$V_i^0 = \sum_{\substack{i \neq j \\ i,j \text{ not bonded}}}^{N} (V_i' \cap v_i) \quad (6)$$

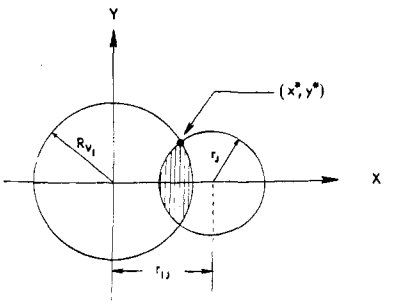

Figure 1. A two-dimensional projection of the geometry of the intersection of the solvation shell of atom i and the van der Waals sphere of atom j.

Since the solvation free energy is, in terms of this model, the change in free energy in going from a completely solvated state to some partially solvated state dictated by conformation K, the total solvation free energy, $F(K)_i$, associated with atom i in the Kth conformation is

$$F(K)_i = \Delta f\left[n - \left(\frac{V_i^0}{V_s + V_f}\right)\right] \text{ when } V_i^0 < n(V_s + V_f) \quad (7)$$

$$F(K)_i = 0 \text{ when } V_i^0 \geq n(V_s + V_f) \quad (8)$$

where n, Δf, and V_f are chosen according to which type of atom is indicated by the index i.

From the way $F(K)_i$ is defined in eq 7 and 8, it is clear that $F(K)_i$ is discontinuous for $V_i^0 = n(V_s + V_f)$. However, since we are considering the intersection of spheres with spheres, V_i^0 will never equal $n(V_s + V_f)$ unless there is a steric overlap of the van der Waals spheres. Under such conditions the conformational energy will be exceedingly high and the entire structure will be rejected. Hence, this polymer–solvent model has continuous energy functions for all "sterically" allowed polymer conformations and can be used without fear of "blow ups" in any minimization routine.

The total solvation free energy, $F_T(K)$, for the macromolecule in the Kth conformation is simply

$$F_T(K) = \sum_{1=i}^{N} F(K)_i \quad (9)$$

Computational Methods. The calculations were done using polypeptide chains 20 residues in length. Only interactions between pairs of atoms less than 12 Å apart were included in the potential energy calculations. The same conformational potential functions and parameters which were used to evaluate the polymer–solvent parameters were also used in these conformational potential energy calculations. Reference 11 describes the choice of potential functions and states where detailed descriptions of the various functions and parameters may be found.

The peptide backbone geometry suggested by Pauling and Corey[15] was used for all amino acid residue polymers. The poly-L-proline bonding geometry was chosen to be identical with that reported by Sasisekharan.[16] The side-chain geometry of some of the amino acid residues contains groups in which the bond angles and bond distances vary considerably. Hence, unless the specific geometry of a side chain is known, it is very probable that errors will be introduced into the calculations. However, the conformational po-

(15) L. Pauling, R. B. Corey, and H. R. Branson, *Proc. Nat. Acad. Sci. U. S.*, 37, 205 (1951).
(16) V. Sasisekharan, *Acta Crystallogr.*, 12, 897 (1959).

TABLE II
THE INITIAL VALUES OF ϕ, ψ, AND χ_1 USED IN THE CONFORMATIONAL ENERGY MINIMIZATIONS OF THE VARIOUS SECONDARY STRUCTURES OF THE VARIOUS HOMOPOLYPEPTIDES

Conformation	ϕ, deg	ψ, deg	χ_1, deg
Right-handed α helix	130	120	60,180,300
Antiparallel β "helix"	60	320	60,180,300
Poly-L-proline II helix	120	325	60,180,300
Extended charged-form helix	30	10	60,300

tential functions are not sufficiently refined so as to require extremely precise side-chain geometries. In other words, the errors introduced by the conformational potential functions negate any gain in accuracy which might result from knowing the precise geometry of the side chains. All side-chain geometries used in the calculations reported here were based upon the bond distances and bond angles suggested by Dickerson and Geis.[17]

The conformational-dependent thermodynamic quantities $\langle A \rangle$, $\bar{E}$, and $\langle S \rangle$ were calculated by minimizing the total conformational energy using some initial conformations of the homopolypeptide. The initial ϕ, ψ, and χ_1 for the various conformations studied in this research are listed in Table II. Values for χ_2, χ_3, and χ_4 are not listed because they vary among the homopolypeptides whose side chains are large enough to possess such rotations. The values assigned to these side-chain rotations were chosen from side-chain conformations of CPK molecular models which "looked" very stable.

The equivalence condition (*i.e.*, ϕ, ψ, and χ of each residue are respectively identical) was invoked. This was done in order to simulate the behavior of a long homopolypeptide chain which is "locally" uniform in conformation. That is, the homopolypeptide chain may not be uniform in conformation for the totality of the chain, but is very nearly uniform in conformation for several of the nearest-neighbor residues. This is probably a very reasonable restriction to impose as long as the conformational simulation of a random coil is not attempted. A random-rotation minimization procedure was employed in the calculations. That is, the values of the ϕ, ψ, and $\{\chi\}$ were varied in a random manner (subject to the constraint of the equivalence condition) such that the absolute values of the maximum possible changes in the values of the rotations were (a) $|\Delta\phi| = 10°$, $|\Delta\psi| = 10°$, $|\{\Delta\chi\}| = 30°$ for the first set of runs and (b) $|\Delta\phi| = 20°$, $|\Delta\psi| = 20°$, $|\{\Delta\chi\}| = 60°$ for the second set of runs.

Whenever a variation in ϕ, ψ, and $\{\chi\}$ resulted in a lowering of the total conformational energy (as compared to the previous low in conformational energy), all gradients in energy dependent upon ϕ, ψ, and $\{\chi\}$ were calculated. If all gradients were positive, a minimum was assumed and a new initial conformation for a particular secondary structure was assigned. If any gradient was negative the random variation of ϕ, ψ, and $\{\chi\}$ continued, with this new low-energy conformation serving as the "previous" low-energy structure mentioned above. Any conformation corresponding to a higher energy than the previously known low-energy conformation was eliminated from further consideration in the energy minimization. This procedure was employed in each of the two runs mentioned above. Each run consisted of 80 iterations; this was sufficient for locating at least two relative minima for each secondary structure tested. Thus, the approximate partition function (calculated for $T = 298°K$) used to compute the thermodynamic properties of a particular secondary structure of a particular homopolypeptide is based upon 160 conformations. It is to be emphasized that the relative minima calculated are not known with sufficient precision to merit discussion of their detailed structures and, secondly, there is no way of knowing whether or not any one of the minima corresponds to the deepest minimum in conformational energy which is associated with a particular secondary structure. ϕ and ψ of any minimum are only known to within $\pm 10°$ and $\{\chi\}$ is known to only $\pm 30°$. The goal in this work was not to locate all of the relative minima associated with a particular secondary structure of a particular homopolypeptide with a high degree of accuracy, but rather to devise a procedure to scan that region in conformational hyperspace associated with a particular secondary structure in order to accurately estimate the partition function associated with the secondary structure.

(17) R. E. Dickerson and I. Geis in "The Structure and Action of Proteins," Harper and Row, New York, N. Y., 1969.

TABLE III
A GROUPING OF THE HOMOPOLYPEPTIDES STUDIED IN THIS REPORT WITH RESPECT TO CHEMICAL CHARACTERISTICS AND SIZE OF SIDE CHAIN

Chemical characterization	Homopolypeptide	Bulk size of side chain
Acidic	Aspartic acid charged	Medium
	Aspartic acid neutral	Medium
	Glutamic acid charged	Large
	Glutamic acid neutral	Large
Neutral	Serine	Small
Neutral hydrophilic	Lysine neutral	Large
	Lysine charged	Large
Hydrophobic	Valine	Medium
	Proline	Large
Neutral basic hydrophilic	Histidine neutral	Large
	Histidine charged	Large

Results

The homopolypeptides investigated in the course of the research reported in this paper are listed in Table III. Also, in Table III, the homopolypeptides are grouped according to the chemical characteristics of the side chains as suggested by Dickerson[17] and the bulk size of the side chains. From an examination of Table III it can be seen that a representative sampling of various types of side chains has been chosen.

Table IV lists the Helmholtz conformational free energy, $\langle A \rangle$, the average conformational internal energy, $\bar{E}$, and the conformational entropy, $\langle S \rangle$, of the homopolypeptides for various secondary structures in aqueous solution and *in vacuo*. The change in these thermodynamic variables in going to aqueous solution from vacuum is also listed. As pointed out by Flory,[18] the thermodynamic variables cannot be calculated precisely since the partition function is calculated using a discrete set of conformations, and also the set of discrete conformations may not contain the major contributions to the partition function. The validity of the results presented in this paper is dependent upon the assumption that the partition function associated with any secondary structure of a homopolypeptide can be well approximated by using an ensemble of conformational energies which are determined by the random-rotation minimization procedure presented above.

(18) P. J. Flory in "Conformation of Biopolymers," Vol. 1, G. N. Ramachandran, Ed., Academic Press, London, 1967, p 339.

TABLE IV
FREE ENERGIES $\langle A \rangle$, AVERAGE INTERNAL ENERGIES $\bar{E}$, AND ENTROPIES $\langle S \rangle$ ASSOCIATED WITH DIFFERENT CONFORMATIONS OF SEVERAL HOMOPOLYPEPTIDES[a]

	$\langle A \rangle$, kcal/mol of residue			$\bar{E}$, kcal/mol of residue			$\langle S \rangle$, cal/(mol of residue deg)		
	Aqueous solution	Vacuum	ΔA (PS)	Aqueous solution	Vacuum	$\Delta \bar{E}$ (PS)	Aqueous solution	Vacuum	ΔS (PS)
Poly-L-alanine									
α_R[b]	−5.5	−5.4	−0.1	−4.3	−4.4	+0.1	3.56	3.40	0.16
β ∦[c]	−3.4	−3.1	−0.3	−1.6	−1.2	−0.4	5.94	6.57	−0.63
PPII[d]	−4.2	−3.6	−0.6	−2.5	−1.6	−0.9	5.68	6.31	−0.63
Poly-L-proline									
PPII	−1.7	−1.1	−0.6	0.0	0.5	−0.5	5.74	5.29	−0.45
Poly-L-valine									
α_R	12.3	11.7	+0.6	12.3	11.7	+0.6	0.00	0.00	0.00
β ∦	−2.0	−2.3	+0.3	−0.9	−1.3	+0.4	3.75	3.78	−0.03
PPII	0.9	0.0	+0.9	1.9	0.8	+1.1	3.03	2.50	+0.53
ECF[e]	−2.7	−2.9	+0.2	−1.6	−1.8	+0.2	3.74	3.73	+0.01
Poly-L-serine									
α_R	−0.3	+2.5	−2.8	−0.0	2.8	−2.8	0.90	1.03	−0.13
β ∦	−3.9	−0.3	−3.6	−3.2	0.3	−4.1	2.29	2.05	+0.24
PPII	−2.7	+0.8	−3.5	−2.1	1.3	−3.3	1.85	1.47	+0.38
Poly(L-aspartic acid) Neutral Form									
α_R	−19.5	−5.1	−14.4	−19.3	−4.8	−14.5	0.67	1.03	−0.36
β ∦	−18.8	+0.5	−19.3	−18.4	+1.3	−19.7	1.57	2.86	−1.29
PPII	−19.3	−1.6	−17.7	−18.9	−1.1	−17.8	1.39	1.88	−0.49
ECF	−14.2	+1.2	−15.4	−13.9	+1.4	−15.3	0.94	0.73	−0.12
Poly(L-aspartic acid) Charged Form									
α_R	−7.8	+19.8	−27.6	−7.5	+20.2	−27.7	1.05	1.25	−0.20
β ∦	−1.4	+22.3	−23.7	−0.7	+22.9	−23.6	2.09	2.19	−0.10
PPII	+4.7	+26.7	−22.0	−5.3	+27.6	−22.3	1.95	3.08	−1.13
ECF	+3.6	+24.5	−20.9	+4.3	+25.1	−20.8	2.44	1.95	+0.49
Poly(L-glutamic acid) Neutral Form									
α_R	−0.3	+12.1	−12.4	+0.2	12.7	−12.9	1.46	2.45	−0.99
β ∦	1.7	+17.1	−18.9	+0.6	20.1	−20.7	3.55	4.03	−0.48
PPII	1.6	−17.1	−18.7	+0.4	20.2	−20.6	3.61	5.27	−1.66
ECF	1.4	+16.8	−18.2	+0.2	20.0	−20.2	3.77	5.95	−21.8
Poly(L-glutamic acid) Charged Form									
α_R	−4.1	+20.0	−24.1	−3.6	+21.0	−25.6	1.50	3.40	−1.90
β ∦	−12.4	+11.8	−24.2	−11.5	+13.1	−24.6	3.22	4.15	−0.93
PPII	−15.7	+10.6	−26.3	−14.6	+12.2	−26.8	3.50	5.40	−19.0
ECF	−20.9	+9.0	−20.9	−19.8	+10.7	−30.5	3.51	5.60	−2.09
Poly-L-histidine Neutral Form									
α_R	−8.8	−7.6	−1.2	−8.3	−7.1	−1.2	1.41	1.41	0.00
β ∦	−6.8	−4.8	−2.0	−6.2	−4.2	−2.0	2.00	2.11	−0.11
PPII	−6.5	−4.5	−2.0	−6.0	−4.1	−1.9	1.74	1.65	+0.09
Poly-L-histidine Charged Form									
α_R	+2.3	+7.4	−5.1	2.9	8.0	−5.1	1.95	1.90	0.05
α ∦	−2.8	+4.2	−7.0	−2.2	4.9	−7.1	2.10	2.50	−0.40
PPII	−3.5	−3.1	−6.6	−2.9	3.8	−6.7	1.98	2.25	−0.27
ECF	−1.6	+5.3	−6.9	−0.9	6.0	−6.9	2.40	2.43	−0.03
Poly-L-lysine Neutral Form									
α_R	−5.8	−5.2	−0.6	−4.5	−4.0	−0.5	4.15	3.95	−0.20
β ∦	−0.9	−0.2	−0.7	+0.7	1.5	−0.8	5.41	5.68	−0.27
PPII	+0.3	+1.0	−1.0	+2.0	3.0	−1.0	4.85	6.40	−0.55
ECF	−0.4	+0.7	−1.1	+1.3	2.4	+1.1	5.76	6.13	−0.37
Poly-L-lysine Charged Form									
α_R	−1.1	+6.5	−7.6	0.0	7.6	−7.6	3.65	3.50	+0.15
β ∦	−2.3	+5.8	−8.1	−0.8	7.5	−8.3	5.13	5.71	−0.58
PPII	−3.7	+4.3	−8.0	−2.1	6.0	−8.1	5.41	5.83	−0.42
ECF	−1.9	+6.0	−7.9	−0.5	7.5	−8.0	4.70	5.02	−0.32

[a] $\langle A \rangle$, $\bar{E}$, and $\langle S \rangle$ are given for both aqueous solution and vacuum. The changes in free energies, ΔA(PS), average internal energies, $\Delta \bar{E}$(PS), and entropies, ΔS(PS), in going from the vacuum to aqueous solution are also listed. The temperature was fixed at 298°K. [b] Right-handed α helix. [c] Antiparallel β sheet. [d] Poly-L-proline II helix. [e] Extended charged-form helix.

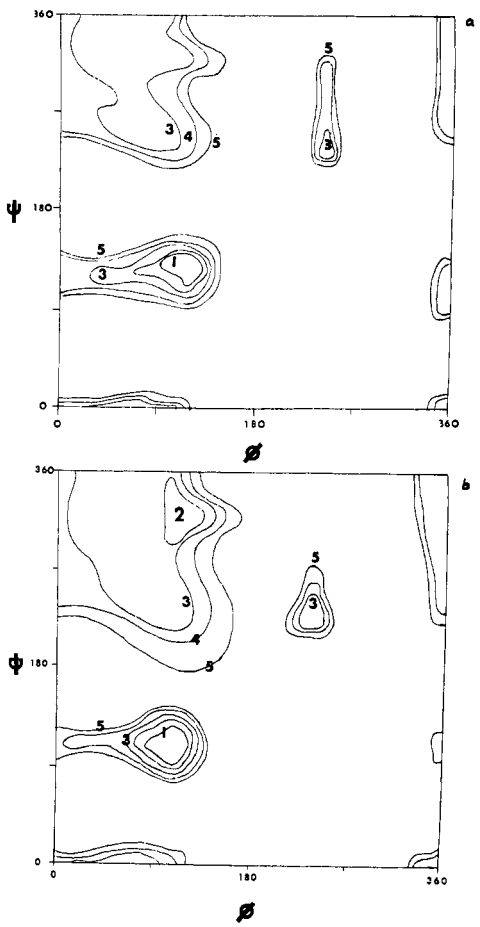

Figure 2. Conformational energy maps of poly-L-alanine. The energy contours (in kilocalories per mole of residue) are extrapolated from a grid in which the conformational energy was minimized with respect to χ_1 (rotation about the C^α–C^β bond) at 10° intervals for both ϕ and ψ. In each of the maps the absolute minimum in energy is assigned a value of zero. The convention of J. T. Edsall, *et al.*, *Biopolymers*, **4**, 121 (1966), is used for defining ϕ and ψ. (a) Poly-L-alanine with aqueous solution interactions neglected. (b) Poly-L-alanine with aqueous solution interactions included.

Keeping this in mind, the following generalizations have been drawn from the data given in Table IV.

(a) For polar solvents, such as water, the interactions of polar groups in the macromolecule with solvent molecules are much more stabilizing than the hydrophobic group interactions with solvent are destabilizing. Poly-L-valine has a destabilization free energy in aqueous solution (as compared to vacuum) of about 0.5 kcal/mol of residue, while poly(L-aspartic acid) in the neutral form has a stabilization free energy in aqueous solution (as compared to a vacuum) of around 17 kcal/mole of residue.

(b) The change in polymer–solvent free energy in going from a polar solvent to vacuum (neutral solvent) is roughly proportional to the solubility of the polymer. Those homopolypeptides which have charged side chains are most soluble. The higher the hydrophobic character of the homopolypeptide, the lower the solubility. Poly-L-proline in form II probably should have a higher ΔA(PS) in view of its known high solubility in aqueous solution. This suggests that the Δf's used to describe the carbonyl carbon and oxygen polymer–solvent interactions should be different for imino acids from the Δf's used for carbonyl and oxygen polymer–solvent interactions used for amino acids.

(c) The polymer–solvent interaction free energy is dependent upon the conformation of the polypeptide backbone and the size and chemical nature of the peptide side chain. Poly-L-alanine would be more soluble (in aqueous solution) in a PPII conformation than in a right-handed α helix. However, from a comparison of the conformational free energies it can be seen that right-handed α helix is statistically more probable. Thus, maximum water solubility of poly-L-alanine is diminished by conformational restrictions.

(d) the polymer–solvent interactions (for aqueous solution and homopolypeptides) do not change the ranking of the conformations of nonionizable homopolypeptides with respect to stability relative to the vacuum calculations. However, the statistical weights associated with observing the various conformations is sensitive to polymer–solvent interactions. In general, the right-handed α helix becomes less probable, while the other conformations become more probable when aqueous solution–homopolypeptide interactions are included in the calculations. Figures 2a and 2b are conformational (ϕ, ψ) maps for poly-L-alanine based on vacuum calculations and aqueous solution–homopolypeptide calculations, respectively. The vacuum conformational map of poly-L-alanine (Figure 2a) differs slightly from those given by other workers. The reason for this is that the conformational potential functions used in this work are slightly different from the sets of functions used by other workers. The region in the upper left-hand corner of the map increases in stability for aqueous solution–poly-L-alanine interactions at the expense of the right-handed α helical region, $\phi = 120°$, $\psi = 120°$. Thus, if one attempts to use conformational calculations to predict Boltzmann average properties of a homopolypeptide (*i.e.*, spectra, transition temperatures) in aqueous solution, it is important to be sure that the polymer–solvent interactions are included in the computations. Hence, Aebersold and Pysh[19] were not able to accurately predict the statistical average CD spectra of various homopolypeptides probably because they neglected polymer–solvent interactions and not because of major errors in the conformational potential functions. Lastly, polymer–solvent interactions may cause changes in the conformations of heteropolypeptide chains which contain a mixture of polar and hydrophobic groups (*i.e.*, proteins) and are in aqueous solution. The effects of polymer–solvent interactions are maximized under these conditions.

(e) Aqueous solution–homopolypeptide interactions play a dominant role, along with intramolecular side chain–side chain interactions, in inducing conformational transitions (right-handed α helix $\rightleftharpoons$ random coil) in homopolypeptides having ionizable side chains. No attempt was made to calculate the thermodynamic properties of the random-coil states of the homopolypeptides which have ionizable side chains. However, the relative stability of the right-handed α helix in the neutral form and the relative instability of this secondary structure in the charged form (as compared to the stability of the other secondary structures studied in this report) indicates that a transition from the right-handed α helix to some new conformation is highly probable. The poly-L-proline II helix, PPII, the antiparallel β sheet "helix," β_R, and the extended charged form helix, ECF, are *not* used as models for a random coil in this analysis of the helix $\rightleftharpoons$ coil transition. (The ECF conformation corresponds to a nearly extended polypeptide chain having $\phi \simeq 30°$ and $\psi \simeq 10°$.) The conformational energies of these secondary structures are used in a comparison with the conformational

(19) D. Aebersold and E. S. Pysh, *J. Chem. Phys.*, **53**, 2156 (1970).

energy of the right-handed α helix (for a particular homopolypeptide) for the sole purpose of demonstrating the relative stability or instability of the right-handed α helix. It is possible that the PPII secondary structure, and/or the ECF secondary structure, might be stable intermediate conformations in the helix $\rightleftharpoons$ coil transition. The ECF conformation was first proposed by Krimm.[20] We have just completed a rather exhaustive study of the helix $\rightleftharpoons$ coil transition in poly(L-glutamic acid) and conclude that ECF is a stable intermediate conformation for this polymer.[21] The data presented in Table IV suggest a helix $\rightleftharpoons$ coil transition for poly-L-histidine as a function of protonation as first suggested by Beychok, *et al.*[22] Further, the most stable side-chain conformation found for the right-handed α helix has side-chain–side chain hydrogen bonds of the type N···H···N formed between residues n and $n + 3$. Infrared studies by Muehlinghaus and Zundel[23] also suggest such hydrogen bonding. One rather surprising result is that poly(L-aspartic acid) should *not* readily undergo a helix $\rightarrow$ coil transition upon deprotonation. The side-chain carboxyl groups are too close to backbone carbonyl oxygens in all but the right-hand α helix to produce a highly destabilizing interaction. Thus, the absence of the single CH_2 unit in the aspartic acid side-chain residue is sufficient to give this homopolypeptide very different properties from poly(L-glutamic acid) which contains the additional CH_2 group. There is some evidence[24–26] which suggests that poly(L-aspartic acid) does not easily undergo the helix $\rightleftharpoons$ coil transition. Poly-L-lysine appears to energetically want to undergo a helix $\rightleftharpoons$ coil transition upon protonation. For all ionizable homopolypeptides, except aspartic acid, the maximizing of the distance between unfavorable side chain–side chain interactions and the maximizing of the exposure of polar groups of the side chains to the aqueous solution induce the helix $\rightleftharpoons$ coil transition.

(20) S. Krimm and J. Mark, *Proc. Nat. Acad. Sci. U. S.*, **60**, 1122 (1968).
(21) W. Hiltner, A. G. Walton, and A. J. Hopfinger, submitted for publication.
(22) S. Beychok, M. N. Pflumm, and J. E. Lehmann, *J. Amer. Chem. Soc.*, **79**, 5227 (1957).
(23) J. Muehlinghaus and G. Zundel, *Biopolymers*, **10**, 711 (1971).

Summary

The polymer–solvent hydration shell model presented in this paper for aqueous solution interactions with homopolypeptides yields results consistent with limited experimental data. This model accounts for hydrophobic and hydrophilic bonding, is sensitive to changes in molecular conformation, and is one of the only polymer–solvent models which can be efficiently employed in existing computer algorithms. Extension of the model to include other solvents such as chloroform seems in order in view of the results presented in this report. Inclusion of a temperature dependence into the model would also be useful, since the small size of the solvent molecules makes their dynamic behavior quite temperature sensitive.

Acknowledgment. I am pleased to acknowledge the support, in part, of this work by a National Institute of Dental Research Grant under Program Project No. DE2587.

(24) A. Berger and E. Katchalski, *J. Amer. Chem. Soc.*, **73**, 4084 (1951).
(25) F. Ascoli and C. Botre, *Biopolymers*, **1**, 353 (1963).
(26) A. L. Jacobson, *ibid.*, **3**, 249 (1965).

Statistical Treatment of the Intramolecular Reaction between Two Functional Groups Connected by a Polymethylene Chain

Masahiko Sisido

Department of Polymer Chemistry, Kyoto University, Kyoto, Japan.
Received June 1, 1971

ABSTRACT: In the reaction between two functional groups of $X\text{-}(CH_2)_{n-2}Y$ type molecules, the intramolecular reaction rate constant may be directly proportional to the probability of the distance r between X and Y being smaller than a given value r_0. This probability for n from 6 to 16 was estimated using a rotational isomer model, multiplying an appropriate statistical weight for each conformational state. Then, the cyclization constant, *i.e.*, the ratio of rate constants for intramolecular and intermolecular reactions, was evaluated and compared with experimental values in the esterification of ω-oxy acids reported by Stoll and Rouvé. If all kinds of long-range interactions were ignored, or conformations in which nonbonded skeletal atoms are situated closer than 1.53 Å were rejected, the calculated cyclization constants showed poor agreement with the observed values. However, if the conformations having skeletal overlaps in which the carbon–carbon distance is less than 2.77 Å were rejected, the calculated values agreed well with the observed ones. It was also found that the reasonable value of r_0 was 2.3–2.7 Å, and using these values, the observed alternating property in the cyclization constants was explained.

The dependence of intramolecular reaction rates in $X\text{-}(CH_2)_{n-2}Y$ type molecules upon the number n of the skeletal atoms has been studied by many workers. Among these studies are papers concerning thermal cyclization of dibasic acids,[1] cyclic ketone formation from dinitriles,[2,3] acid-catalyzed lactone formation from ω-oxy acids,[4] etc. In the last example, Stoll and Rouvé[4] determined the cyclization constant, *i.e.*, the ratio of rate constants for intramolecular, k_1, and intermolecular, k_2, reactions. Their values were recalculated by the method developed by Morawetz and Goodman,[5] and are plotted in Figure 1. In this figure, the yield of the intramolecular reaction product in the cyclic ketone for-

(1) L. Ruzicka, W. Brugger, M. Pfeiffer, H. Schinz, and M. Stoll, *Helv. Chim. Acta*, **9**, 499 (1926).
(2) K. Ziegler and R. Aurnhammer, *Justus Liebigs Ann. Chem.*, **513**, 43 (1934).
(3) K. Ziegler and W. Hechelhammer, *ibid.*, **528**, 114 (1937).
(4) M. Stoll and A. Rouvé, *Helv. Chim. Acta*, **18**, 1087 (1935).
(5) H. Morawetz and N. Goodman, *Macromolecules*, **3**, 699 (1970).